

Pincer-Type Heck Catalysts and Mechanisms Based on Pd^{IV} Intermediates: A Computational Study

Olivier Blacque and Christian M. Frech^{*[a]}

Abstract: Pincer-type palladium complexes are among the most active Heck catalysts. Due to their exceptionally high thermal stability and the fact that they contain Pd^{II} centers, controversial Pd^{II}/Pd^{IV} cycles have been often proposed as potential catalytic mechanisms. However, pincer-type Pd^{IV} intermediates have never been experimentally observed, and computational studies to support the proposed Pd^{II}/Pd^{IV} mechanisms with pincer-type catalysts have never been carried out. In this computational study the feasibility of potential catalytic cycles involving Pd^{IV} intermediates was explored. Density functional calculations were performed on experimentally applied aminophosphine-, phosphine-, and phosphite-based pincer-type Heck catalysts with styrene and phenyl bromide as substrates and (*E*)-stilbene as coupling product. The potential-energy surfaces were calculated in dimethylformamide (DMF) as solvent and demonstrate that Pd^{II}/Pd^{IV} mechanisms are thermally accessible and thus a true alternative

to formation of palladium nanoparticles. Initial reaction steps of the lowest energy path of the catalytic cycle of the Heck reaction include dissociation of the chloride ligands from the neutral pincer complexes $[(2,6\text{-C}_6\text{H}_3\text{(XPR}_2)_2)\text{Pd}(\text{Cl})]$ [$\text{X}=\text{NH}$, $\text{R}=\text{piperidynyl}$ (**1a**); $\text{X}=\text{O}$, $\text{R}=\text{piperidynyl}$ (**1b**); $\text{X}=\text{O}$, $\text{R}=\text{iPr}$ (**1c**); $\text{X}=\text{CH}_2$, $\text{R}=\text{iPr}$ (**1d**)] to yield cationic, three-coordinate, T-shaped $14e^-$ palladium intermediates of type $[(2,6\text{-C}_6\text{H}_3\text{(XPR}_2)_2)\text{Pd}]^+$ (**2**). An alternative reaction path to generate complexes of type **2** (relevant for electron-poor pincer complexes) includes initial coordination of styrene to **1** to yield styrene adducts $[(2,6\text{-C}_6\text{H}_3\text{(XPR}_2)_2)\text{Pd}(\text{Cl})(\text{CH}_2=\text{CHPh})]$ (**4**) and consecutive dissociation of the chloride ligand to yield cationic square-planar styrene com-


plexes $[(2,6\text{-C}_6\text{H}_3\text{(XPR}_2)_2)\text{Pd}(\text{CH}_2=\text{CHPh})]^+$ (**6**) and styrene. Cationic styrene adducts of type **6** were additionally found to be the resting states of the catalytic reaction. However, oxidative addition of phenyl bromide to **2** result in pentacoordinate Pd^{IV} complexes of type $[(2,6\text{-C}_6\text{H}_3\text{(XPR}_2)_2)\text{Pd}(\text{Br})(\text{C}_6\text{H}_5)]^+$ (**11**), which subsequently coordinate styrene (in *trans* position relative to the phenyl unit of the pincer cores) to yield hexacoordinate phenyl styrene complexes $[(2,6\text{-C}_6\text{H}_3\text{(XPR}_2)_2)\text{Pd}(\text{Br})(\text{C}_6\text{H}_5)(\text{CH}_2=\text{CHPh})]^+$ (**12**). Migration of the phenyl ligand to the olefinic bond gives cationic, pentacoordinate phenylethenyl complexes $[(2,6\text{-C}_6\text{H}_3\text{(XPR}_2)_2)\text{Pd}(\text{Br})(\text{CHPhCH}_2\text{-Ph})]^+$ (**13**). Subsequent β -hydride elimination induces direct HBr liberation to yield cationic, square-planar (*E*)-stilbene complexes with general formula $[(2,6\text{-C}_6\text{H}_3\text{(XPR}_2)_2)\text{Pd}(\text{CHPh=CHPh})]^+$ (**14**). Subsequent liberation of (*E*)-stilbene closes the catalytic cycle.

Keywords: density functional calculations • Heck reaction • palladium • pincer complexes • reaction mechanisms

Introduction

Palladium-catalyzed arylation of alkenes (Heck reaction) is nowadays one of the most important methods for carbon-carbon bond formation, which finds application in all areas of organic chemistry, ranging from the laboratory bench through the synthesis of pharmaceutical fine chemicals to the production of bulk chemicals.^[1] Various types of palladium complexes are known to promote this transformation, of which many follow the “classical” Pd⁰/Pd^{II} mechanism,^[2] for example, as is the case for $[\text{Pd}(\text{PPh}_3)_2(\text{OAc})_2]$ or $[\text{Pd}(\text{PPh}_3)_4]$.^[3] Other systems, such as $[\text{Pd}(\text{OAc})_2]$, serve as sour-

[a] Dr. O. Blacque, Dr. C. M. Frech
Department of Inorganic Chemistry
University of Zürich
8057 Zürich (Switzerland)
Fax: (+41) 44-635-6802
E-mail: chfrech@aci.uzh.ch

 Supporting information (energies and Cartesian coordinates of all calculated intermediates and transition states) for this article is available on the WWW under <http://dx.doi.org/10.1002/chem.200902091>.

ces of palladium nanoparticles.^[4] Pincer-type complexes, which were introduced as Heck catalysts in the late 1990s, still belong to the most active catalysts and continuously attract attention because of their unique balance between stability and reactivity. Seemingly slight electronic and steric modifications have been demonstrated to dramatically influence their catalytic activities.^[5–7] Primarily due to their exceptionally high thermal stability and the fact that they contain Pd^{II} centers, controversial Pd^{II}/Pd^{IV} cycles have been proposed as potential catalytic mechanisms.^[8] Although recent experimental and computational investigations indicated that aminophosphine-based pincer-type Pd^{IV} intermediates can be traversed in halide exchange reactions,^[7b] such species have never been experimentally observed in even one of the known pincer systems. On the other hand, it was recently demonstrated that aminophosphine- and phosphite-based pincer complexes serve as stable and clean sources of palladium nanoparticles,^[6b,p] and also xylene-derived systems (homogeneous species as well as complexes immobilized on soluble and insoluble supports) were found to decompose under Heck reaction conditions when organic bases such as triethylamine were used.^[9,10] Moreover, transformations of the above mentioned pincer-type Heck catalysts into homogeneous Pd⁰ complexes under Heck reaction conditions was recently excluded.^[7b] Even though all these results seemingly indicate that palladium nanoparticles are the catalytically active form of any type of pincer Heck catalyst, the possibility that some of the modifications might lead to a change of mechanism cannot be excluded completely. Remarkably, even though Pd^{II}/Pd^{IV} cycles were often proposed as potential catalytic mechanisms, computational studies on pincer-type complexes have never been performed to support this assumption. Therefore, to find out whether pincer-type Heck catalysts which can catalyze the arylation of olefins via Pd^{II}/Pd^{IV} mechanisms exist, we carried out computational studies on experimentally applied amino-phosphine-, phosphine- and phosphite-based pincer-type Heck catalysts.

We show that pincer-type Pd^{IV} intermediates are thermally accessible in polar, nonprotic solvents at a reaction temperature of 140 °C, and consequently catalytic cycles with the Pd^{II}/Pd^{IV} redox pair are a true alternative to the formation of palladium nanoparticles.^[11] Moreover, seemingly slight modifications of the pincer core and/or phosphine substituents proved to have a significant impact on

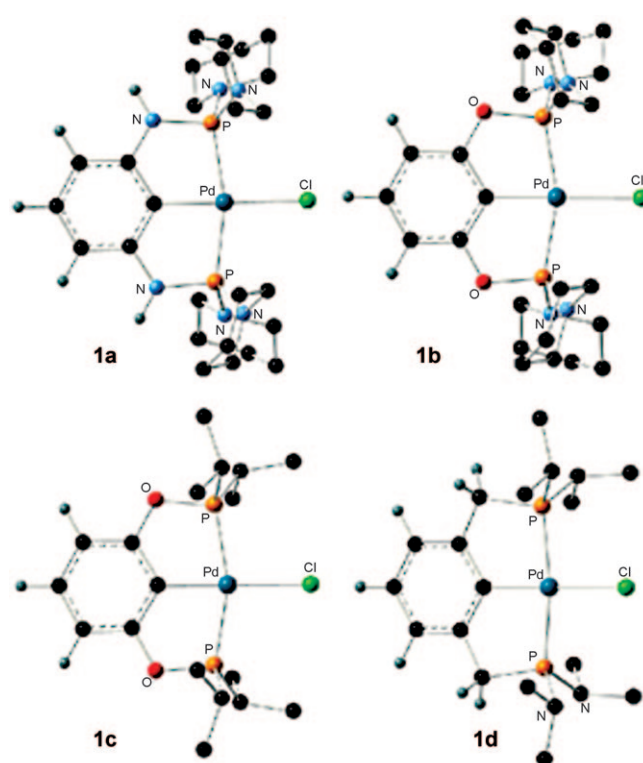


Figure 1. DFT optimized structures of the experimentally applied pincer-type Heck catalysts $[[2,6\text{-C}_6\text{H}_3(\text{XPR}_2)_2]\text{Pd}(\text{Cl})]$ [X=NH, R = piperidinyl (**1a**); X=O, R = piperidinyl (**1b**); X=O, R = *i*Pr (**1c**); X=CH₂, R = *i*Pr (**1d**)] selected for this computational study. Selected hydrogen atoms are omitted for clarity.

Table 1. Calculated electronic energies E_e , solvation energies $\Delta_{\text{sol}}E$, ZPE corrections, and reaction energies Δ_rE in the gas phase and in dimethylformamide for the studied mechanisms.^[a]

System	X=NH, R=piperidinyl					
	$E_e(\text{g})$ [hartree]	gas phase ZPE(g) [hartree]	$\Delta_rE(\text{g})$ [kcal mol ⁻¹]	$E_e(\text{sol})$ [hartree]	in dimethylformamide $\Delta_{\text{sol}}E$ [kcal mol ⁻¹]	$\Delta_rE(\text{sol})$ [kcal mol ⁻¹]
1	–2617.112504	+0.715020	0.0	–2617.136413	–15.0	0.0
2	–2156.659290	+0.714053	+124.0	–2156.716762	–36.1	+23.8
3	–5420.230562	+0.80878	+23.2	–5420.257612	–17.0	+25.4
3'	–5420.205806	+0.807986	+38.2	–5420.225435	–12.3	+45.1
4	–2926.639102	+0.852298	+26.9	–2926.670146	–19.5	+26.8
5	–2926.586553	+0.849058	+57.8	–2926.610279	–14.9	+62.3
6	–2466.260063	+0.852410	+105.0	–2466.315992	–35.1	+10.2
7	–2926.628091	+0.851899	+6.7	–2926.654268	–16.4	+9.7
8	–2926.535667	+0.847757	+62.1	–2926.562554	–16.9	+64.7
9	–5729.738951	+0.943105	+59.6	–5729.758514	–12.3	+71.0
10	–2466.155044	+0.847044	+167.5	–2466.211561	–35.5	+72.3
11	–4959.808798	+0.807591	+127.3	–4959.870274	–38.6	+28.8
12	–5269.363986	+0.945450	+136.6	–5269.421279	–36.0	+45.1
13	–5269.423241	+0.946906	+100.3	–5269.483719	–38.0	+6.9
14	–2697.251297	+0.934222	+104.9	–2697.312236	–38.2	+6.3
TS_{1/3}	–5420.169157	+0.807400	+60.8	–5420.195748	–16.7	+63.4
TS_{1/3'}	–5420.162893	+0.806923	+64.4	–5420.181834	–11.9	+71.8
TS_{2/11}	–4959.788543	+0.806708	+139.4	–4959.845596	–35.8	+43.7
TS_{4/5}	–2926.569900	+0.846884	+66.9	–2926.595066	–15.8	+70.5

[a] $E_e(\text{g})$ is the electronic energy in the gas phase, $E_e(\text{sol})$ the electronic energy in solution, $\Delta_{\text{sol}}E$ the calculated solvation energy, $\Delta_rE(\text{g})$ the reaction energy in the gas phase corrected for ZPE, and $\Delta_rE(\text{sol})$ the reaction energy in solution corrected for ZPE.

Table 2. Calculated electronic energies E_e , solvation energies $\Delta_{\text{sol}}E$, ZPE corrections, and reaction energies Δ_rE in the gas phase and in dimethylformamide for the studied mechanisms.^[a]

System	X = O, R = piperidinyl					
	gas phase	in dimethylformamide				
	$E_e(\text{g})$ [hartree]	ZPE(g) [hartree]	$\Delta_rE(\text{g})$ [kcal mol ⁻¹]	$E_e(\text{sol})$ [hartree]	$\Delta_{\text{sol}}E$ [kcal mol ⁻¹]	$\Delta_rE(\text{sol})$ [kcal mol ⁻¹]
1	-2656.854455	+0.691014	0.0	-2656.870968	-10.4	0.0
2	-2196.392619	+0.689620	+129.1	-2196.444990	-32.9	+27.5
4	-2966.383867	+0.828251	+25.1	-2966.410181	-16.5	+23.3
6	-2505.997993	+0.827994	+107.2	-2506.050578	-33.0	+9.9
11	-4999.540120	+0.783490	+133.9	-4999.593133	-33.3	+36.1
12	-5309.098869	+0.920841	+140.6	-5309.150277	-32.3	+48.2
13	-5309.157236	+0.921462	+104.4	-5309.210450	-33.4	+10.9
14	-2736.991902	+0.909348	+105.2	-2737.044851	-33.2	+6.9
TS_{2/11}	-4999.511826	+0.781403	+150.3	-4999.562450	-31.8	+54.0

System	X = O, R = <i>i</i> Pr					
	gas phase	in dimethylformamide				
	$E_e(\text{sol})$ [hartree]	$\Delta_{\text{sol}}E$ [kcal mol ⁻¹]	$\Delta_rE(\text{sol})$ [kcal mol ⁻¹]	$E_e(\text{sol})$ [hartree]	$\Delta_{\text{sol}}E$ [kcal mol ⁻¹]	$\Delta_rE(\text{sol})$ [kcal mol ⁻¹]
1	-2125.849799	+0.467820	0.0	-2125.864496	-9.2	0.0
2	-1665.376479	+0.465993	+136.1	-1665.432946	-35.4	+30.7
4	-2435.368336	+0.605211	+32.0	-2435.395927	-17.3	+28.3
6	-1974.981924	+0.604169	+114.0	-1975.037354	-34.8	+13.7
11	-4468.524442	+0.560146	+140.7	-4468.579025	-34.3	+40.8
12	-4778.080057	+0.697816	+149.6	-4778.135531	-34.8	+53.5
13	-4778.144668	+0.699293	+110.0	-4778.201208	-35.5	+13.2
14	-2205.979799	+0.686791	+110.3	-2206.035389	-34.9	+9.2
TS_{2/11}	-4468.503945	+0.558637	+152.6	-4468.557285	-33.5	+53.5

System	X = CH ₂ , R = <i>i</i> Pr					
	gas phase	in dimethylformamide				
	$E_e(\text{g})$ [hartree]	ZPE(g) [hartree]	$\Delta_rE(\text{g})$ [kcal mol ⁻¹]	$E_e(\text{g})$ [hartree]	ZPE(g) [hartree]	$\Delta_rE(\text{g})$ [kcal mol ⁻¹]
1	-2054.022704	+0.515673	0.0	-2054.039128	-10.3	0.0
2	-1593.564965	+0.514517	+126.7	-1593.619381	-34.1	+23.7
4	-2363.547062	+0.652971	+28.3	-2363.574776	-17.4	+25.6
6	-1903.160347	+0.652902	+111.1	-1903.213918	-33.6	+13.1
11	-4396.713088	+0.608786	+131.3	-4396.770995	-36.3	+30.4
12	-4706.269787	+0.747310	+140.1	-4706.326104	-35.3	+44.6
13	-4706.325892	+0.747998	+105.3	-4706.383982	-36.5	+8.7
14	-2134.160978	+0.735948	+105.9	-2134.214587	-33.6	+7.2
TS_{2/11}	-4396.685055	+0.607467	+148.1	-4396.740217	-34.6	+48.9

System	Reactants			
	gas phase	in dimethylformamide		
	$E_e(\text{g})$ [hartree]	ZPE(g) [hartree]	$E_e(\text{sol})$ [hartree]	$E_e(\text{sol}) + \text{ZPE(g)}$ [hartree]
Cl ⁻	-460.254652	–	-460.380787	-460.380787
HCl	-460.797420	+0.006828	-460.806319	-460.799491
HBr	-2572.157923	+0.006056	-2572.165816	-2572.159760
H ₂ C=CHPh	-309.566934	+0.134813	-309.573980	-309.439167
PhHC=CHPh	-540.573862	+0.217207	-540.586394	-540.369187
C ₆ H ₅ Br	-2803.152964	+0.091774	-2803.159743	-2803.067969
C ₆ H ₅ Cl	-691.791702	+0.092141	-691.798515	-691.706374

[a] $E_e(\text{g})$ is the electronic energy in the gas phase, $E_e(\text{sol})$ is the electronic energy in solution, $\Delta_{\text{sol}}E$ is the calculated solvation energy, $\Delta_rE(\text{g})$ is the reaction energy in the gas phase corrected for ZPE, and $\Delta_rE(\text{sol})$ is the reaction energy in solution corrected for ZPE.

the energies of intermediates and transition states traversed in the Heck reaction, in accordance with the expected trend: the higher the electron density on the metal center, the lower the ground-state energy and energetic barrier.

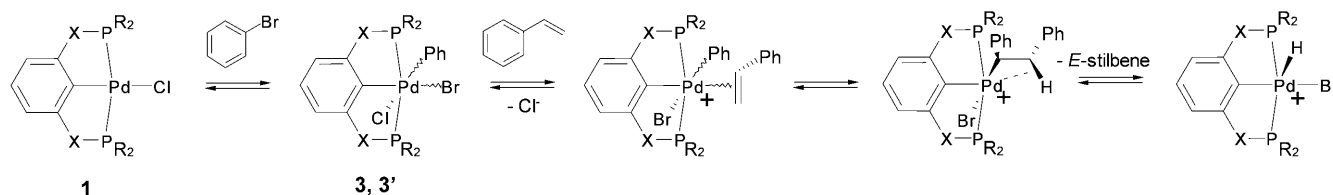
P(piperidinyl)₂ or PiPr_2 groups (Figure 1) with styrene and phenyl bromide as substrates and (*E*)-stilbene as coupling product. Various reaction paths involving Pd^{IV} intermediates and transition states were calculated in order to find out whether Pd^{II}/Pd^{IV} mechanisms are thermally accessible with

Computational Details

Geometry optimizations and frequency calculations for all reactants, intermediates, products, and transition states were performed at the density functional level of theory by using the Gaussian 03 program package with the *m*PW1PW91 hybrid functional,^[12] which includes modified Perdew–Wang exchange and Perdew–Wang 91 correlation,^[13] in conjunction with the Stuttgart/Dresden ECPs (SDD) basis set for the Pd center,^[14] the standard 6-31G basis set for the hydrogen atoms,^[15] and the polarized 6-31G(d) basis set for the remaining atoms.^[16] Pure basis functions (5d, 7f) were used in all calculations. Geometries were fully optimized without symmetry restrictions, and transition-state structures were obtained by using the QST2 procedure.^[17] For each optimized stationary point a frequency analysis was performed to verify its character (minimum or saddle point). For transition states we carefully checked that the vibrational mode associated to the imaginary frequency corresponds to the correct movement. In addition, single-point calculations were carried out for all optimized gas-phase geometries by using the CPCM polarizable conductor calculation model.^[18] Dimethylformamide (DMF) was chosen as solvent of reaction and explicitly specified with a dielectric constant ϵ of 38.3. Then, the zero-point energy (ZPE) corrections obtained from the gas-phase frequency calculations were included in all relative energies in the gas phase $\Delta E(\text{g})$ and in solution $\Delta E(\text{sol})$.

Results and Discussion

Density functional calculations were performed on the experimentally applied aminophosphine-, phosphite-, and phosphine-based pincer-type Heck catalysts $[[2,6\text{-C}_6\text{H}_3\text{-}(\text{XPR}_2)_2]\text{Pd}(\text{Cl})]$ [X = NH, R = piperidinyl (**1a**); X = O, R = piperidinyl (**1b**); X = O, R = *i*Pr (**1c**); X = CH₂, R = *i*Pr (**1d**)] bearing sterically demanding



Scheme 1. Possible catalytic cycle of the Heck reaction, initiated by direct oxidative addition of phenyl bromide to **1a**. **a**: X = NH and R = piperidinyl; **b**: X = O and R = piperidinyl; **c**: X = O and R = *i*Pr; **d**: X = CH₂ and R = *i*Pr.

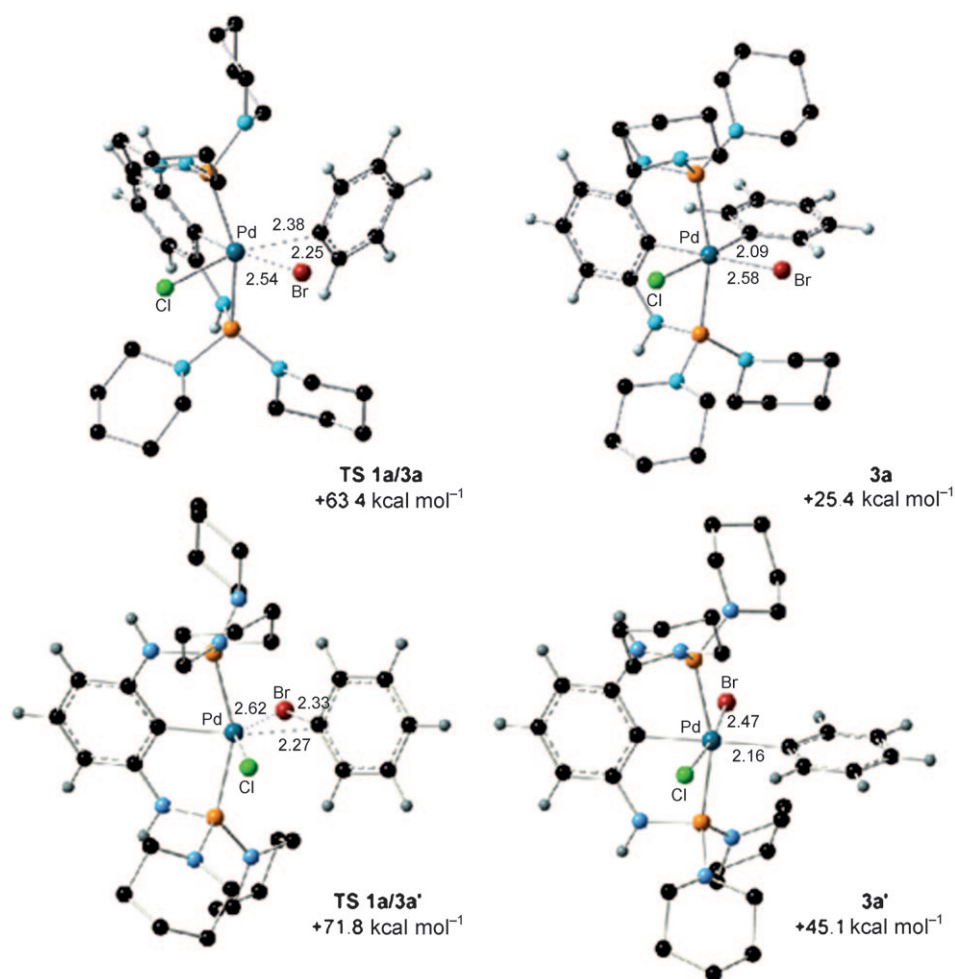


Figure 2. DFT geometrical details and relative energies of the transition states **TS_{1a/3a}** and **TS_{1a/3a'}** as well as the minima **3a** and **3a'** along the oxidative addition of phenyl bromide to the neutral Pd^{II} center of **1a** (bond lengths are in angstroms and energies are relative to the ground-state reactants).

pincer-type Heck catalysts and hence could be a true alternative to formation of palladium nanoparticles.

Pincer complexes have several possibilities to catalyze the arylation of olefins via Pd^{II}/Pd^{IV} mechanisms, all of which are initiated by styrene coordination or oxidative addition of phenyl bromide either to neutral, square-planar 16e⁻ complexes of type **1** or to cationic, T-shaped 14e⁻ complexes of type **2**. All of these possible initiation steps, as well as the subsequent

transformations, were preliminarily investigated with **1a** (Table 1), the most electron rich pincer complex used in this study (and hence that for which the most favorable energies for Pd^{IV} intermediates and the corresponding transition states were expected to be obtained),^[19] as we anticipated that if the calculated reaction steps are thermally inaccessible with **1a**, the mechanism also could not be accessed by the other systems.^[21] The energetically most favorable reaction paths were then re-calculated with all of the other pincer complexes (Table 2) in order to find out whether Pd^{IV} intermediates are thermally accessible in at least one of the selected systems and how strong the influence of the modifications on the ground-state energies and the transition states is.

Although seemingly less likely, a possible catalytic cycle of the Heck reaction could be initiated by oxidative addition of phenyl bromide to **1** to give the neutral, six-coordinate phenyl pincer complexes of type $[[2,6\text{-C}_6\text{H}_3\text{-(XPR}_2)_2]\text{Pd(Br)(Cl)(C}_6\text{H}_5)]$ (**3**) with the metal center in the oxidation state of +IV, similar to

the recently reported coupling of alkenes with iodonium salts, for which the involvement of six-coordinate Pd^{IV} intermediates was postulated (and supported by DFT calculations).^[22] However, subsequent halide dissociation, coordination of styrene (in *cis* position relative to the phenyl ligand), and migration of the phenyl ligand to the olefinic bond would yield the cationic, pentacoordinate 1,2-diphenylethyl complexes, which could undergo β-hydride elimination and liberate (*E*)-stilbene, for example, to give cationic hydride

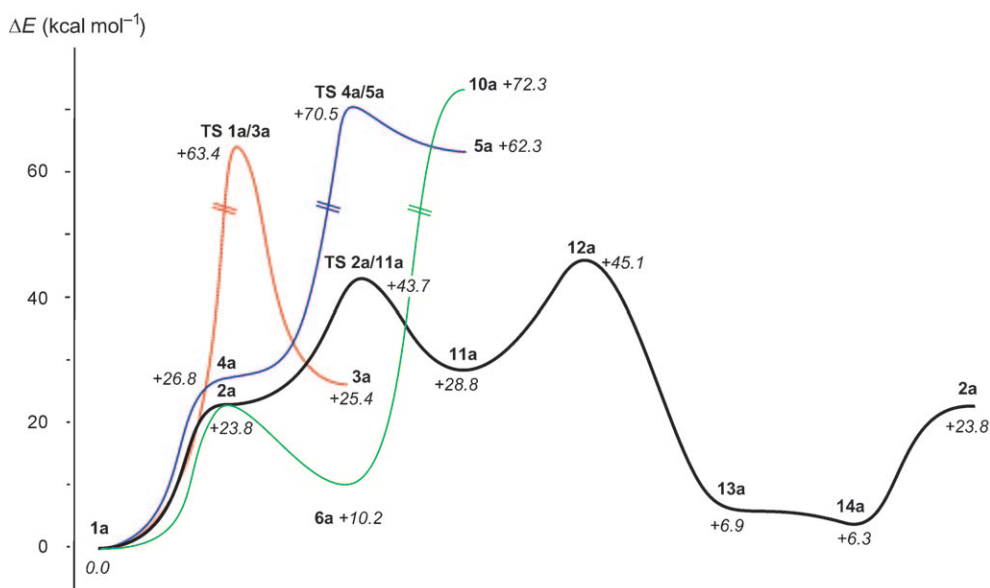
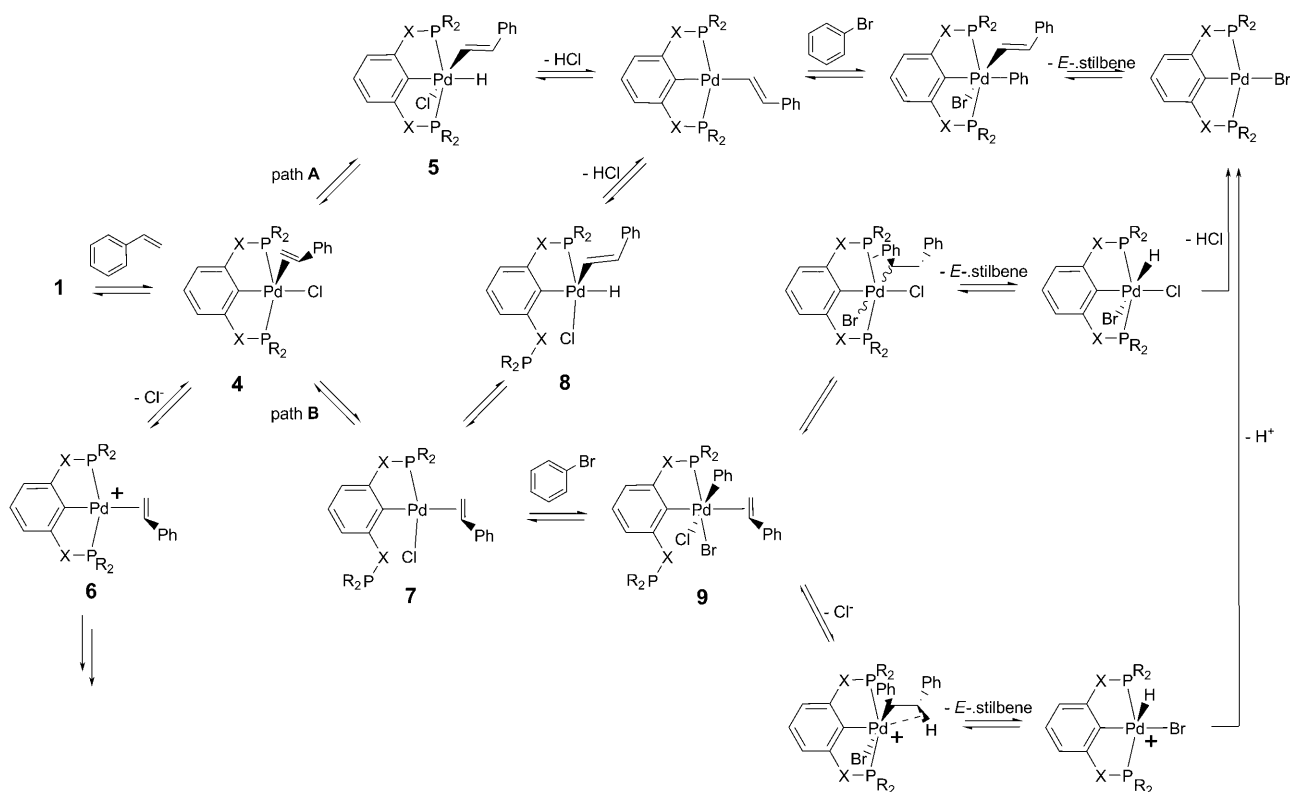


Figure 3. Potential-energy surfaces for the calculated reactions of **1a** with styrene and/or phenyl bromide. Energies are in kcal mol⁻¹ and relative to the ground-state reactants.



Scheme 2. Possible catalytic cycles of the Heck reaction evaluated for **1a**. **a**: X=NH and R=piperidinyl; **b**: X=O and R=piperidinyl; **c**: X=O and R=iPr; **d**: X=CH₂ and R=iPr.

complexes of type $[[2,6\text{-C}_6\text{H}_3(\text{XPR}_2)_2]\text{Pd}(\text{halide})(\text{H})]^+$. The catalytic cycle could be closed after their deprotonation (Scheme 1).^[23]

The oxidative addition of phenyl bromide to **1a** to yield **3a** is initiated by a Pd–Br interaction, leading to a three-

centered transition state **TS**_{1a/3a} with distorted trigonal-bipyramidal geometry around the metal center (Figure 2). The transition state (**TS**_{1a/3a}) is characterized by significant elongation of the Br–C bond by 0.36 Å (Br–C 2.25 Å) and a relative *trans* position of the phenyl group with respect to the

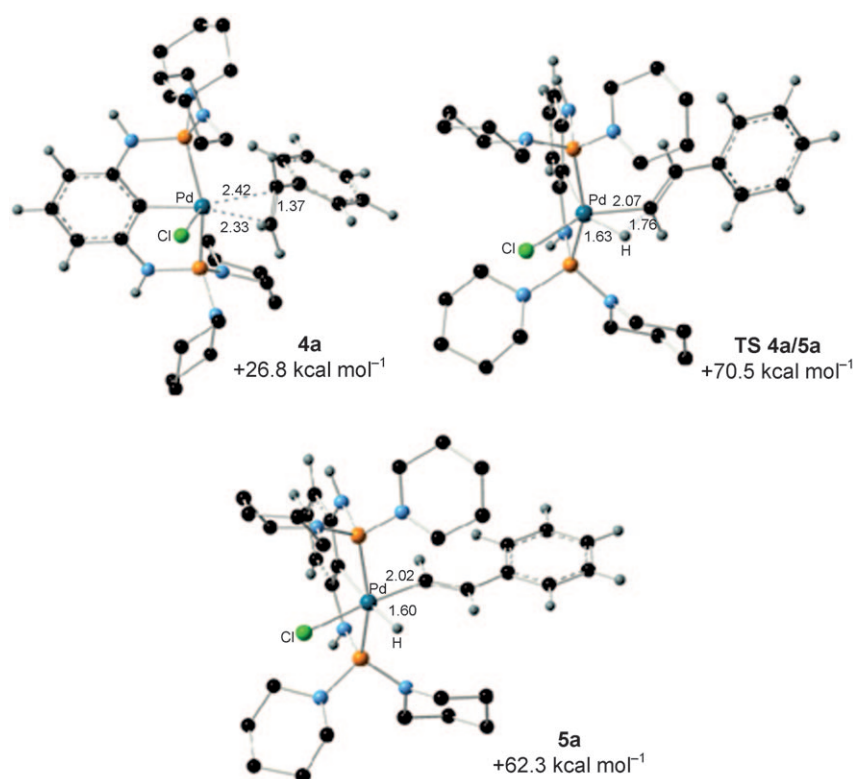


Figure 4. DFT geometrical details and relative energies of transition state $\text{TS}_{4a/5a}$ and minima **4a** and **5a**. Bond lengths are in angstrom and energies are relative to the ground-state reactants.

chloride ligand ($\text{Br-Pd-Cl } 145.5^\circ$), while the phenyl ring lies perpendicular to the equatorial plane between the halogen atoms. The activation energy for $\text{TS}_{1a/3a}$ is calculated to be $63.4 \text{ kcal mol}^{-1}$ relative to the ground-state energies of the isolated reactants (Figure 3). Thus, even though subsequent Br–C bond breakage and formation of octahedral complex **3a** with the palladium center in the oxidation state of +IV is stabilized by $38.0 \text{ kcal mol}^{-1}$ relative to $\text{TS}_{1a/3a}$ (the ground-state energy of **3a** is $25.4 \text{ kcal mol}^{-1}$), the oxidative addition process and formation of **3a** is thermally not accessible. The situation is the same for its structural isomer **3a'** (with the phenyl ligand in *trans* position relative to the aromatic pincer core), which has a significantly higher ground-state energy than **3a** (the ground-state energy of **3a'** is $45.1 \text{ kcal mol}^{-1}$) and an energetic barrier of $71.8 \text{ kcal mol}^{-1}$ above the energy of the ground-state reactants ($\text{TS}_{1a/3a'}$) (Figure 2 and 3). Consequently, the Heck reaction cannot be initiated by direct oxidative addition of aryl bromides to pincer complexes of type **1**, and therefore subsequent transformations involving **3a** or **3a'** were not investigated further.

Other catalytic mechanisms which could be envisaged to be operative in the Heck reaction are initiated by coordination of styrene to **1** and formation of neutral, square-pyramidal complexes of type $[(2,6\text{-C}_6\text{H}_3(\text{XPR}_2)_2)\text{Pd}(\text{Cl})(\text{CH}_2=\text{CHPh})]$ (**4**). Subsequent reaction steps could either include oxidative addition of the vinyl C–H bond of coordinated

styrene (to yield phenylethenyl hydride complexes of type **5**), HCl elimination followed by the oxidative addition of phenyl bromide, and reductive elimination of (*E*)-stilbene, as was recently suggested by Shaw and co-workers (path **A** in Scheme 2),^[24] chloride dissociation to yield cationic, square-planar styrene adducts of type $[(2,6\text{-C}_6\text{H}_3(\text{XPR}_2)_2)\text{Pd}(\text{CH}_2=\text{CHPh})]^+$ (**6**) and further reaction steps^[25] or, seemingly less likely, dissociation of one of the phosphine arms to yield neutral, square-planar styrene complexes of type **7** (path **B**, Scheme 2), which either could undergo oxidative addition of the vinyl C–H bond of styrene to yield phenylethenyl hydride complexes of type **8** and merge into reaction path **A**, or oxidatively add phenyl bromide to give the neutral, hexacoordinate phenyl pincer complexes with the general formula $[(2,6\text{-C}_6\text{H}_3(\text{XPR}_2)_2)\text{Pd}(\text{Br})(\text{Cl})(\text{CH}_2=\text{CHPh})(\text{C}_6\text{H}_5)]$ (**9**). Subsequent

migration of the phenyl ligand to the olefinic bond, β -hydride elimination (either prior to phosphine re-coordination or after halide dissociation), accompanied by liberation of the coupling product and HX ($\text{X}=\text{halide}$) elimination from the neutral palladium hydride complexes of type $[(2,6\text{-C}_6\text{H}_3(\text{XPR}_2)_2)\text{Pd}(\text{Br})(\text{Cl})(\text{H})]$ or deprotonation from its cationic analogues, respectively, could close the catalytic cycles (see Scheme 2).

However, even if the coordination of styrene to **1a** to form adduct **4a** (Figure 4) is endothermic by $26.8 \text{ kcal mol}^{-1}$ and thus could indeed be a possible intermediate in the catalytic cycle of the Heck reaction, oxidative addition of the vinyl C–H bond and formation of the palladium phenylethenyl hydride complex $[(2,6\text{-C}_6\text{H}_3\text{-[NHP(piperidiny)]}_2)\text{Pd}(\text{Cl})(\text{H})(\text{CH}=\text{CHPh})]$ (**5a**) cannot occur, since the corresponding energetic barrier (Figure 4) of $70.5 \text{ kcal mol}^{-1}$ relative to the energy of the isolated reactants and $43.7 \text{ kcal mol}^{-1}$ relative to **4a** is far too high for it to be part of the catalytic cycle (Figure 3). Although breakage of the C–H bond would lead to stabilization by $8.2 \text{ kcal mol}^{-1}$ (relative to $\text{TS}_{4a/5a}$), formation of **5a** remains highly endothermic (by $35.5 \text{ kcal mol}^{-1}$ relative to **4a**), and hence this reaction path was also not investigated further.

Similarly, although dissociation of one of the phosphine arms of **4a** and formation of **7a** could possibly occur under catalytic reaction conditions (formation of **7a** is endothermic by $9.7 \text{ kcal mol}^{-1}$),^[26] its formation is not relevant for the

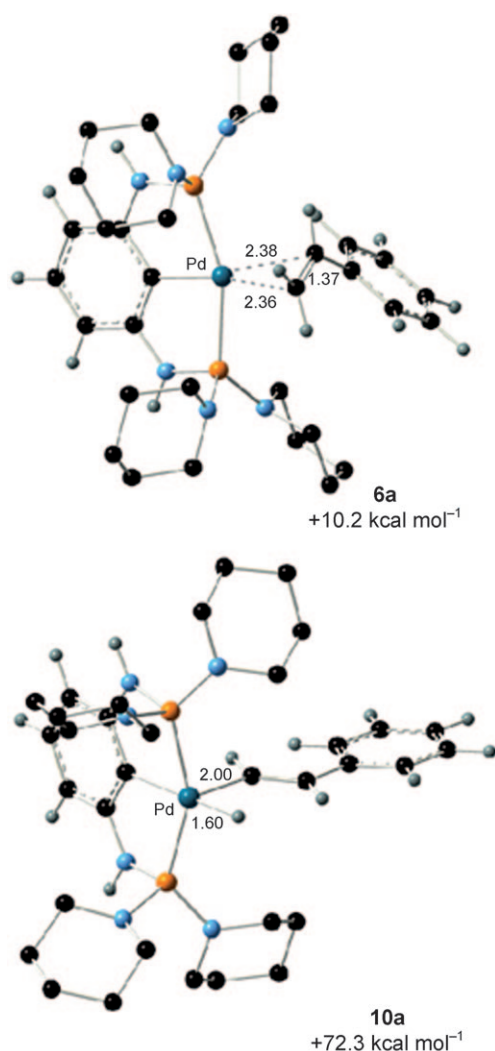


Figure 5. DFT geometrical details and relative energies of minima **6a** and **10a**. Bond lengths are in angstrom and energies are relative to the ground-state reactants.

catalytic cycle, since dissociation of the chloride ligand from **4a** and formation of cationic square-planar styrene adduct $[[2,6\text{-C}_6\text{H}_3(\text{XPR}_2)_2]\text{Pd}(\text{CH}_2=\text{CHPh})]^+$ (**6a**) is thermodynamically and kinetically favored over formation of **7a**,^[27] and hence reaction paths with the involvement of complexes of type **7** are not considered to be part of the catalytic cycle.^[28,29]

Since the oxidative addition of phenyl bromide and oxidative addition of the C–H bond of styrene to **1a** showed very early high-lying transition states, dissociation of the chloride ligand from the square-pyramidal complexes of type **1** prior to oxidative addition of phenyl bromide or coordination of styrene was calculated. Chloride dissociation from **1** yields cationic, T-shaped $14e^-$ complexes with general formula $[[2,6\text{-C}_6\text{H}_3(\text{XPR}_2)_2]\text{Pd}]^+$ (**2**). Optimized complex **2a** exhibits a ground-state, solvent-corrected energy which is 23.8 kcal mol^{−1} higher than the ground-state energies of the reactants. Moreover, subsequent coordination of styrene is exothermic

by 13.6 kcal mol^{−1} and yields cationic square-planar styrene complex $[[2,6\text{-C}_6\text{H}_3(\text{XPR}_2)_2]\text{Pd}(\text{CH}_2=\text{CHPh})]^+$ (**6a**) with a relative ground-state energy of 10.2 kcal mol^{−1}, which implies that cationic styrene complexes of type **6** are present in the reaction mixtures of the Heck reaction, either as an intermediate in the catalytic cycle, or more likely as resting state of the catalytic mechanism, which provides more facile access to cationic intermediates of type **2**. Indeed, complexes of type **6** cannot be intermediates of the catalytic cycle, since oxidative addition of the vinyl C–H bond of styrene and formation of the cationic palladium phenylethenyl hydride complex $[[2,6\text{-C}_6\text{H}_3(\text{XPR}_2)_2]\text{Pd}(\text{H})(\text{CH}=\text{CHPh})]^+$ (**10a**, Figure 5), which after deprotonation could oxidatively add phenyl bromide and thereafter reductively eliminate (*E*)-stilbene, is far too high in energy to be thermally accessible. The ground-state energy of phenylethenyl hydride complex **10a** lies 72.3 kcal mol^{−1} above the ground-state energy of the reactants, and thus it is unnecessary to calculate the corresponding transition state to determine whether **10a** is a possible intermediate in the catalytic cycle of the Heck reaction (Figures 3 and 5).

On the other hand, oxidative addition of phenyl bromide to **2a** to give cationic five-coordinate Pd^{IV} complex $[[2,6\text{-C}_6\text{H}_3(\text{XPR}_2)_2]\text{Pd}(\text{Br})(\text{C}_6\text{H}_5)]^+$ (**11a**) with the phenyl ligand positioned *cis* to the aromatic unit of the pincer core (Figure 6) is only slightly endothermic. Complex **11a** has a computed ground-state energy of only 28.8 kcal mol^{−1}, which is 5.0 kcal mol^{−1} above the sum of the ground-state energies of the reactants. Importantly, the corresponding transition state (**TS**_{2a/11a}) is only 19.9 kcal mol^{−1} higher in energy than calculated for the isolated reactants and thus thermally accessible. Transition state **TS**_{2a/11a} (Figure 6) is mainly characterized by significant elongation of the Br–C bond by 0.58 Å (Br–C 2.47 Å) and a relative *trans* position of the bromide ligand with respect to the pincer unit (*C*_{pincer}–Pd–Br 169.7°). Interaction of the metal center with the *C*_{phenyl} carbon atom (2.16 Å) results in side-on coordination of phenyl bromide, which leads to Br–C bond breakage to yield cationic pentacoordinate bromo phenyl pincer complex **11a**, accompanied by rotation of the phenyl ring, which lies in the equatorial plane. The bromide ligand remains in *trans* position relative to the pincer unit (*C*_{pincer}–Pd–Br 152.6, *C*_{pincer}–Pd–*C*_{phenyl} 84.3°). Subsequent coordination of styrene *trans* to the aromatic unit of the pincer core (*cis* coordination of styrene relative to the phenyl ligand is required for subsequent phenyl migration to the olefinic bond of styrene) yield hexacoordinate $18e^-$ complex $[[2,6\text{-C}_6\text{H}_3(\text{XPR}_2)_2]\text{Pd}(\text{Br})(\text{C}_6\text{H}_5)(\text{CH}_2=\text{CHPh})]^+$ (**12a**) with a relative ground-state energy of 45.1 kcal mol^{−1} (Figure 6). The olefin ligand of **12a** is unsymmetrically bound to the metal center, with carbon atom C1 bearing the phenyl ring 3.19 Å from the palladium center, while the second olefinic carbon atom C2 is closer at 2.70 Å. However, subsequent migration of the phenyl ligand of **12a** to the olefinic bond is strongly exothermic ($\Delta E = 38.2$ kcal mol^{−1}) and yields cationic 1,2-diphenylethyl palladium complex $[[2,6\text{-C}_6\text{H}_3(\text{XPR}_2)_2]\text{Pd}(\text{Br})(\text{CHPhCH}_2\text{Ph})]^+$ (**13a**) with a relative

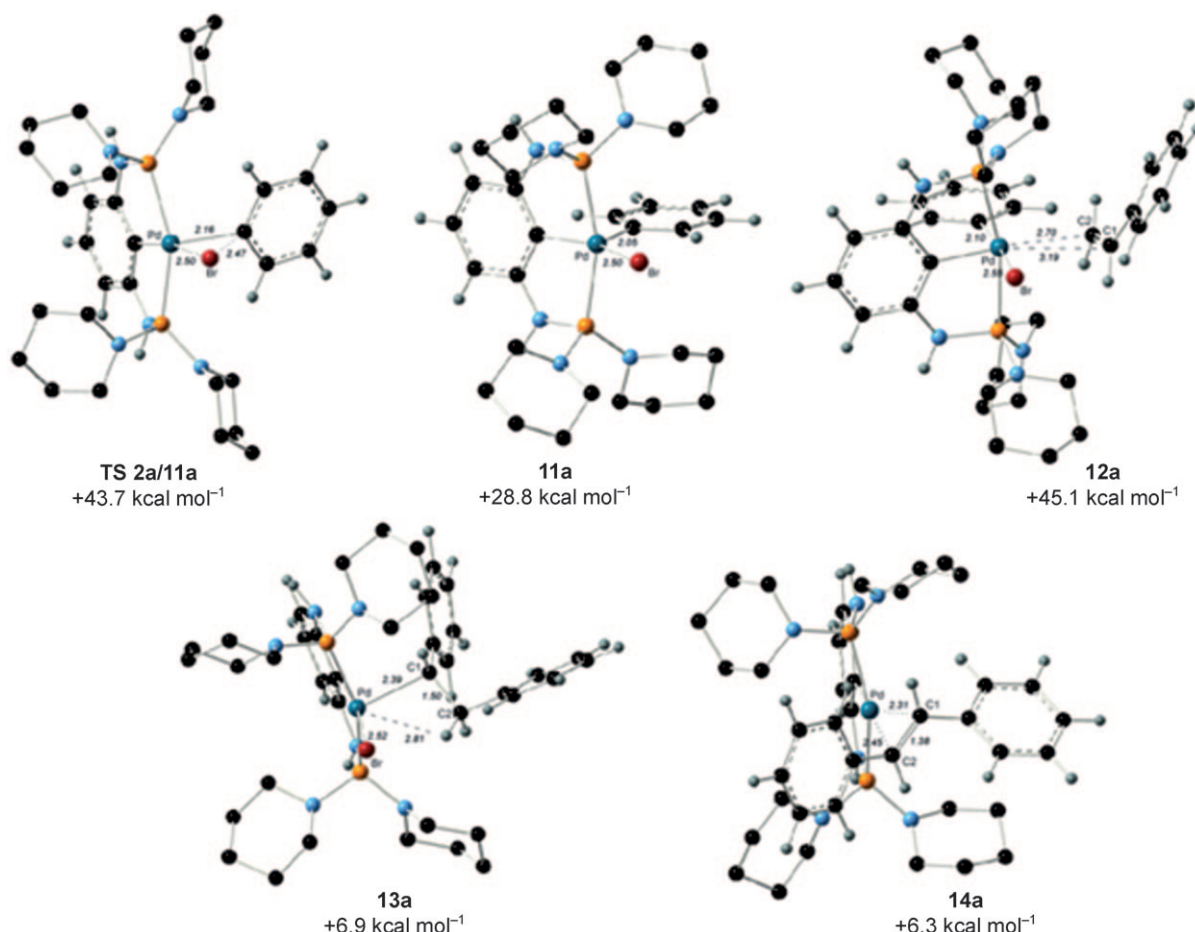


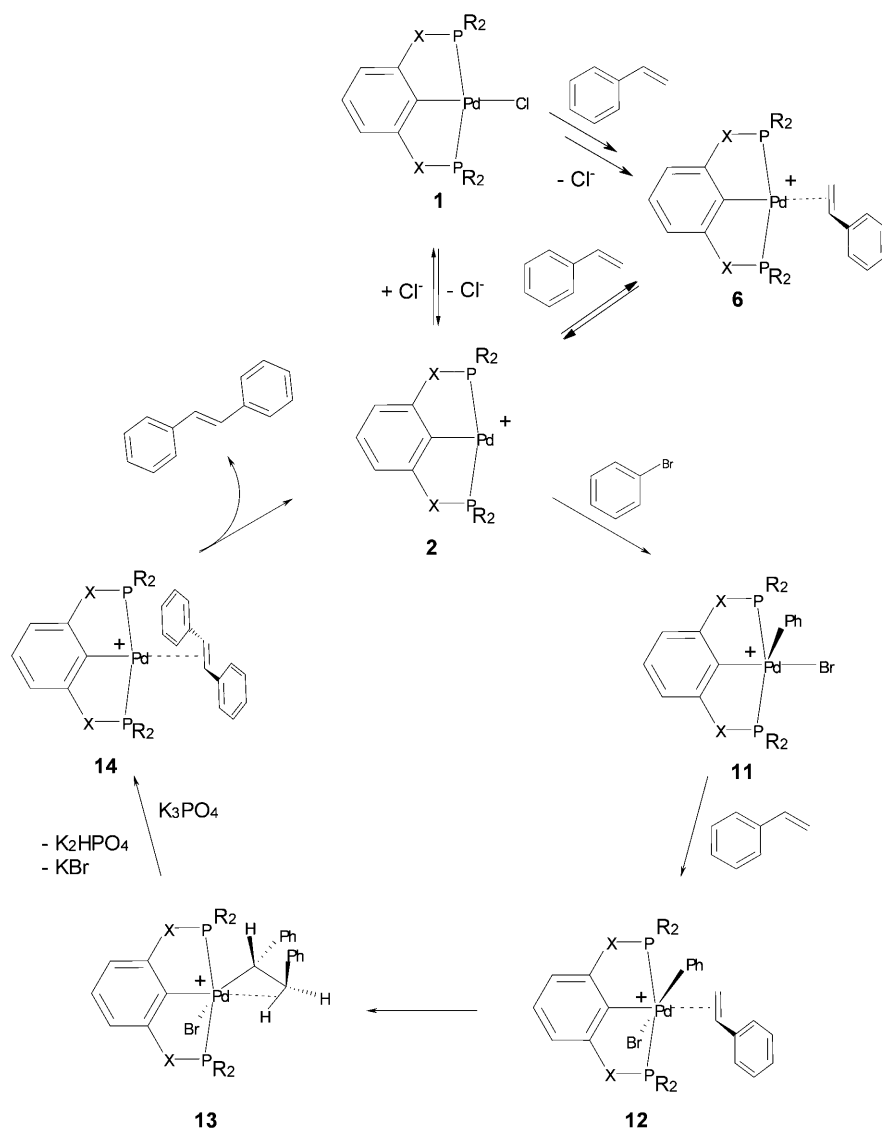
Figure 6. DFT geometrical details and relative energies of transition state **TS_{2a/11a}** and minima **11a**, **12a**, **13a** and **14a**. Bond lengths are in angstrom and energies are relative to **1a** and the ground-state reactants.

ground-state energy of only 6.9 kcal mol⁻¹ (Figure 6). The bromide ligand pushed into *cis* position to the pincer unit by styrene coordination in **12a** recovers a *trans* position (Br-Pd-C_{pincer} 168.0°), since the olefin migrated to the position previously occupied by the phenyl ring. The metal center is stabilized by an agostic interaction of one of the CH₂ hydrogen atoms of the 1,2-diphenylethyl ligand of **13a** (Figure 6), ready for subsequent β-hydride elimination and formation of cationic pincer hydride complex $[[2,6\text{-C}_6\text{H}_3\text{(XPR}_2)_2]\text{Pd(H)(Br)(PhCH=CHPh)}]^+$.

In the course of optimization of pincer hydride complex $[[2,6\text{-C}_6\text{H}_3\text{(XPR}_2)_2]\text{Pd(H)(Br)(PhCH}_2\text{CH}_2\text{Ph)}]^+$, direct HBr elimination occurred to give cationic (*E*)-stilbene complex $[[2,6\text{-C}_6\text{H}_3\text{(XPR}_2)_2]\text{Pd(PhCH=CHPh)}]^+$ (**14a**) with a ground-state energy of 6.3 kcal mol⁻¹. (*E*)-Stilbene liberation from **14a** is endothermic by 17.5 kcal mol⁻¹ and closes the catalytic cycle. The lowest energy reaction path calculated for **1a**, and thus the generally proposed catalytic cycle of the Heck reaction promoted by pincer-type Heck catalysts, is given in Scheme 3.^[30]

Re-calculation of the proposed catalytic mechanism of the Heck reaction given in Scheme 3 for pincer complexes **1b–d** demonstrated that catalytic cycles involving pincer-type Pd^{IV}

intermediates are thermally accessible (in polar, nonprotic solvents at elevated reaction temperatures) and thus a true alternative to the formation of palladium nanoparticles (Figure 7). Seemingly slight modifications of the phosphine residues were shown to have a significant impact on the energies of intermediates and transition states that follows the expected trend: the higher the electron density on the metal center, the lower the ground-state energy and energy barrier. This trend holds for all the reaction steps of the proposed catalytic cycle. For example, whereas chloride dissociation from **1a** and **1d**, the pincer complexes with the highest electron densities on the metal center,^[19] is endothermic by only 23.8 and 23.7 kcal mol⁻¹, respectively, a ground-state energy of 27.5 kcal mol⁻¹ was calculated for **2b**. The highest ground-state energy was calculated for **2c** (30.7 kcal mol⁻¹), the pincer complex with the lowest electron density on the metal center. The situation is the same for the subsequent oxidative addition of phenyl bromide and formation of cationic phenyl pincer complexes of type $[[2,6\text{-C}_6\text{H}_3\text{(XPR}_2)_2]\text{Pd(Br)(Ph)}]^+$ (**11**), which is only slightly endothermic (<10 kcal mol⁻¹) but accompanied by an energetic barrier (**TS_{2/11}**) of 20–25 kcal mol⁻¹. However, even if the coordination of styrene to **2a–d** to form styrene adducts with



Scheme 3. Proposed catalytic cycle of the Heck reaction promoted by pincer-type catalysts involving Pd^{IV} intermediates with cationic styrene complex **6** as resting state. **a**: $X=NH$ and $R=piperidinyl$; **b**: $X=O$ and $R=piperidinyl$; **c**: $X=O$ and $R=iPr$; **d**: $X=CH_2$ and $R=iPr$.

general formula $[[2,6-C_6H_3(XPR_2)_2]Pd(CH_2=CHPh)]^+$ (**6**) is exothermic by 13.6 (**2a**), 17.6 (**2b**), 17.0 (**2c**), and 10.6 kcal mol⁻¹ (**2d**) and hence generally favored over oxidative addition of phenyl bromide to **2a–d**, formation of styrene adducts does not prevent the oxidative addition process. In contrast, the styrene adducts **6a–d** are probably the catalyst resting states, whose formation is particularly beneficial for electron-poor pincer complexes such as **1b** and **1c**, since their styrene adducts provide energetically more favorable access to cationic, T-shaped $14e^-$ complexes of type $[[2,6-C_6H_3(XPR_2)_2]Pd]^+$ (**2**), the key intermediates of the catalytic cycle. Indeed, whereas chloride dissociation from **1a** and **1d** is energetically favored over styrene-adduct formation (by ca. 3 kcal mol⁻¹), initial coordination of styrene and consecutive dissociation of the chloride ligand (to yield the cationic

square-planar styrene complexes $[[2,6-C_6H_3(XPR_2)_2]Pd(CH_2=CHPh)]^+$ (**6**) and styrene are energetically preferred for pincer complexes with lower electron density on the metal center, such as **1b** and **1c** (formation of **4b** and **4c** is endothermic by 23.3 and 28.3 kcal mol⁻¹, respectively, and hence favored over chloride dissociation by 4.2 and 2.4 kcal mol⁻¹, respectively). However, subsequent coordination of styrene to the phenyl pincer complexes of type **11a–d** to form the hexacoordinate phenyl styrene complexes $[[2,6-C_6H_3(XPR_2)_2]Pd(Br)(C_6H_5)(CH_2=CHPh)]^+$ (**12**) are endothermic by only 16.3, 12.1, 12.7, and 14.2 kcal mol⁻¹, respectively. In contrast, migration of the phenyl ligand to the olefinic bond to give the cationic pentacoordinate phenylethenyl complexes $[[2,6-C_6H_3(XPR_2)_2]Pd(Br)(CHPhCH_2P-h)]^+$ (**13**) and subsequent β -hydride elimination, which leads in direct liberation of HBr and thus cationic (*E*)-stilbene complexes $[[2,6-C_6H_3(XPR_2)_2]Pd(PhCH=CHPh)]^+$ (**14**), are highly exothermic (by ca. 40 kcal mol⁻¹) for all derivatives. Subsequent liberation of (*E*)-stilbene regenerates the catalyst and is endothermic by about 20 kcal mol⁻¹.

Conclusions

The feasibility of Pd^{II}/Pd^{IV} mechanisms in the Heck reaction promoted by pincer-type catalysts was computationally investigated on experimentally applied aminophosphine-, phosphine-, and phosphite-based pincer complexes with general formula $[[2,6-C_6H_3(XPR_2)_2]Pd(Cl)]$ [$X=NH$, $R=piperidinyl$ (**1a**); $X=O$, $R=piperidinyl$ (**1b**); $X=O$, $R=iPr$ (**1c**); $X=CH_2$, $R=iPr$ (**1d**)]. The proposed catalytic cycle includes initial formation of cationic, T-shaped complexes of type $[[2,6-C_6H_3(XPR_2)_2]Pd]^+$ (**2**), oxidative addition of phenyl bromide (**11**), and subsequent coordination of styrene in *trans* position relative to the phenyl unit of the pincer core (**12**). Migration of the phenyl ligand to the ole-

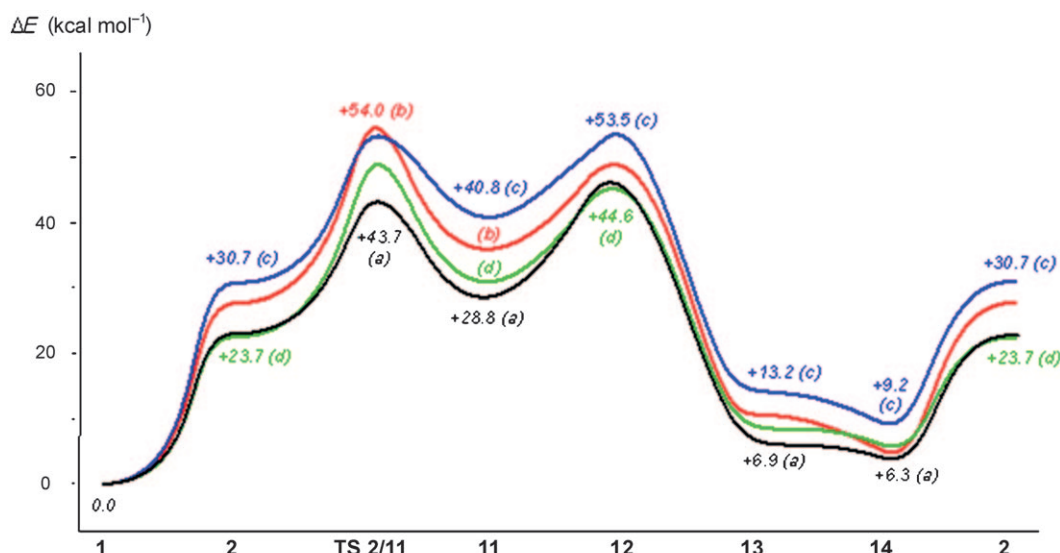


Figure 7. Comparison of the lowest energy path of the Heck coupling of phenyl bromide and styrene to form (*E*)-stilbene promoted by **1a**, **1b**, **1c**, and **1d**.

finic bond (**13**), followed by β -hydride elimination leads to direct liberation of HBr and the cationic, square-planar (*E*)-stilbene complexes of type **14**. The catalyst is regenerated by liberation of (*E*)-stilbene. Our calculations demonstrate that catalytic cycles of the Heck reaction involving Pd^{IV} intermediates are thermally accessible and hence a true alternative to the formation of palladium nanoparticles. The phosphine residues in pincer complexes showed a significant effect on the energies of intermediates and transition states, generally following the expected trend: the higher the electron density on the metal center, the lower the ground state energy and energetic barrier.

However, even if our computational results indicate that mechanisms with the $\text{Pd}^{\text{II}}/\text{Pd}^{\text{IV}}$ redox pair are thermally feasible with pincer-type Heck catalysts, this does not imply that $\text{Pd}^{\text{II}}/\text{Pd}^{\text{IV}}$ mechanisms are operative in any case. In contrast, palladium nanoparticles were recently shown to be the catalytically active form of **1a**, the pincer complex with the highest electron density on the metal center and thus that for which the lowest energy path was calculated. On the other hand, even though palladium nanoparticles are the active form of aminophosphine- (and phosphite-) based pincer complexes, this is not necessarily true for phosphine-based pincer complexes, for which a homogeneous mechanism with Pd^{IV} species may indeed be operative. However, since our computational studies demonstrate that pincer-type Pd^{IV} intermediates are thermally accessible, they must generally be considered as reactive intermediates in reactions performed in polar, nonprotic solvents with aryl halides at elevated temperatures.

Acknowledgements

Financial support of this work by the University of Zurich and the Swiss National Science Foundation (SNSF) are acknowledged.

- [1] For reviews of palladium-catalyzed Heck reaction, see: a) R. F. Heck in *Palladium Reagents in Organic Syntheses* (Eds.: A. R. Katritzky, O. Meth-Cohn, C. W. Rees), Academic Press, London, **1985**, p. 2; b) R. F. Heck in *Comprehensive Organic Synthesis*, Vol. 4 (Eds.: B. M. Trost, I. Fleming), Pergamon, Oxford, **1991**; c) J.-L. Malleron, J.-C. Fiaud, J.-Y. Legros in *Handbook of Palladium-Catalysed Organic Reactions*, Academic Press, London, **1997**; d) M. T. Reetz in *Transition Metal Catalysed Reactions* (Eds.: S. G. Davies, S.-I. Murahashi), Blackwell, Oxford, **1999**; e) J. T. Link, L. E. Overman in *Metal-Catalyzed Cross-Coupling Reactions* (Eds.: F. Diederich, P. J. Stang), Wiley-VCH, Weinheim, **1998**, Chapter 6; f) S. Bräse, A. de Meijere in *Metal-Catalyzed Cross-Coupling Reactions* (Eds.: F. Diederich, P. J. Stang), Wiley, New York, **1998**, Chapter 3.6; g) K. C. Nicolaou, E. J. Sorensen in *Classics in Total Synthesis*, VCH, Weinheim, **1996**; Chapter 31; h) R. A. de Vries, P. C. Vosejka, M. L. Ash in *Catalysis of Organic Reactions* (Ed.: F. E. Herkes) Dekker, New York, **1998**, Chapter 37; i) L. F. Tietze, G. Kettischau, U. Heuschert, G. Nordmann, *Chem. Eur. J.* **2001**, *7*, 368.
- [2] In the “classical” $\text{Pd}^0/\text{Pd}^{\text{II}}$ mechanism, coordinatively unsaturated $14e^- \text{Pd}^0$ complexes of type $[\text{Pd}(\text{PR}_3)_2]$ are assumed to be the catalytically active species, which oxidatively add aryl halides to yield square-planar Pd^{II} intermediates of type $[\text{Pd}(\text{Ar})(\text{X})(\text{PR}_3)_2]$. Dissociation of a ligand (either a phosphine or the halide) provides a coordination site for olefin association, which subsequently can insert into the $\text{Pd}-\text{C}_{\text{aryl}}$ bond to yield a palladium alkyl complex. This intermediate is converted to the reaction product and a palladium hydride complex by β -hydride elimination. The catalyst is regenerated after HX elimination in the presence of a base.
- [3] a) C. Amatore, E. Carre, A. Jutand, *Organometallics* **1995**, *14*, 5605; b) J. F. Fauvarque, F. Pflüger, M. Troupel, *J. Organomet. Chem.* **1981**, *208*, 419.
- [4] G. J. de Vries, *Dalton Trans.* **2006**, 421.
- [5] M. Ohff, A. Ohff, M. E. van der Boom, D. Milstein, *J. Am. Chem. Soc.* **1997**, *119*, 11687.
- [6] a) D. Morales-Morales, R. Redon, C. Yung, C. M. Jensen, *Chem. Commun.* **2000**, 1619; C. Yung, C. M. Jensen, *Chem. Commun.* **2000**,

- 1619; b) E. Peris, J. A. Loch, J. Mata, R. H. Crabtree, *Chem. Commun.* **2001**, 201; c) S. Gründemann, M. Albrecht, J. A. Loch, J. W. Faller, R. H. Crabtree, *Organometallics* **2001**, 20, 5485; d) J. A. Loch, M. Albrecht, E. Peris, J. Mata, J. W. Faller, R. H. Crabtree, *Organometallics* **2002**, 21, 700; e) D. J. Nielsen, K. J. Cavell, B. W. Skelton, A. H. White, *Inorg. Chim. Acta* **2002**, 327, 116; f) W. A. Herrmann, V. P. W. Böhm, C. W. K. Gstöttmayr, M. Grosche, C.-P. Reisinger, T. Weskamp, *J. Organomet. Chem.* **2001**, 617, 616; g) C. Yang, H. M. Lee, S. P. Nolan, *Org. Lett.* **2001**, 3, 1511; h) N. Tsouras, A. A. Danopoulos, A. A. D. Tulloch, M. E. Light, *Organometallics* **2003**, 22, 4750; i) D. Benito-Garagorri, V. Bocokic, K. Mereiter, K. Kirchner, *Organometallics* **2006**, 25, 3817; j) K. Kiewel, Y. Liu, D. E. Bergbreiter, G. A. Sulikowski, *Tetrahedron Lett.* **1999**, 40, 8945; k) F. Miyazaki, K. Yamaguchi, M. Shibasaki, *Tetrahedron Lett.* **1999**, 40, 7379; l) D. Morales-Morales, C. Grause, K. Kasaoka, R. Redon, R. Cramer, C. M. Jensen, *Inorg. Chim. Acta* **2000**, 300–302, 958; m) S. Sjövall, O. P. Wendt, C. Anderson, *J. Chem. Soc. Dalton Trans.* **2002**, 1396; n) D. Morales-Morales, R. E. Cramer, C. M. Jensen, *J. Organomet. Chem.* **2002**, 654, 44; o) M. R. Eberhard, *Org. Lett.* **2004**, 6, 2125; p) N. Whitcombe, K. K. Hii (Mimi), S. Gibson, *Tetrahedron* **2001**, 57, 7449.
- [7] a) J. L. Bolliger, O. Blacque, C. M. Frech, *Angew. Chem.* **2007**, 119, 6634; *Angew. Chem. Int. Ed.* **2007**, 46, 6514; b) J. L. Bolliger, C. M. Frech, *Chem. Eur. J.* **2008**, 14, 7969.
- [8] a) W. A. Herrmann, C. Brossmer, K. Öfele, C.-P. Reisinger, T. Priemeier, M. Beller, H. Fisher, *Angew. Chem.* **1995**, 107, 1989; *Angew. Chem. Int. Ed. Engl.* **1995**, 34, 1844; b) M. Beller, T. H. Riermeier, S. Haber, H.-J. Kleiner, W. A. Herrmann, *Chem. Ber.* **1996**, 129, 1259.
- [9] W. J. Sommer, K. Yu, J. S. Sears, Y. Ji, X. Zheng, R. J. Davis, C. D. Sherrill, C. W. Jones, M. Weck, *Organometallics* **2005**, 24, 4351.
- [10] Whereas decomposition of xylene-derived pincer complexes (and others) was found to occur on performing Heck reactions with organic bases, this is not necessarily the case when inorganic bases such as K_2CO_3 and K_3PO_4 are used.
- [11] Although our results indicate that mechanisms involving a Pd^{III}/Pd^{IV} redox system are thermally accessible for electron-rich pincer-type Heck catalysts, it nevertheless can not be excluded that palladium nanoparticles are their catalytically active form, as it was recently demonstrated to be the case for highly electron-rich aminophosphine-based pincer systems.^[7b]
- [12] Gaussian 03, Revision C.02, M. J. Frisch, G. W. Trucks, H. B. Schlegel, G. E. Scuseria, M. A. Robb, J. R. Cheeseman, J. A. Montgomery, Jr., T. Vreven, K. N. Kudin, J. C. Burant, J. M. Millam, S. S. Iyengar, J. Tomasi, V. Barone, B. Mennucci, M. Cossi, G. Scalmani, N. Rega, G. A. Petersson, H. Nakatsuji, M. Hada, M. Ehara, K. Toyota, R. Fukuda, J. Hasegawa, M. Ishida, T. Nakajima, Y. Honda, O. Kitao, H. Nakai, M. Klene, X. Li, J. E. Knox, H. P. Hratchian, J. B. Cross, V. Bakken, C. Adamo, J. Jaramillo, R. Gomperts, R. E. Stratmann, O. Yazyev, A. J. Austin, R. Cammi, C. Pomelli, J. W. Ochterski, P. Y. Ayala, K. Morokuma, G. A. Voth, P. Salvador, J. J. Dannenberg, V. G. Zakrzewski, S. Dapprich, A. D. Daniels, M. C. Strain, O. Farkas, D. K. Malick, A. D. Rabuck, K. Raghavachari, J. B. Foresman, J. V. Ortiz, Q. Cui, A. G. Baboul, S. Clifford, J. Ciołowski, B. B. Stefanov, G. Liu, A. Liashenko, P. Piskorz, I. Komaromi, R. L. Martin, D. J. Fox, T. Keith, M. A. Al-Laham, C. Y. Peng, A. Nanayakkara, M. Challacombe, P. M. W. Gill, B. Johnson, W. Chen, M. W. Wong, C. Gonzalez, J. A. Pople, Gaussian Inc., Wallingford, CT, **2004**.
- [13] a) C. Adamo, V. Barone, *J. Chem. Phys.* **1998**, 108, 664; b) J. P. Perdew, K. Burke, Y. Wang, *Phys. Rev. B* **1996**, 54, 16533; c) K. Burke, J. P. Perdew, Y. Wang, in *Electronic Density Functional Theory: Recent Progress and New Directions* (Eds.: J. F. Dobson, G. Vignale, M. P. Das), Plenum Press, New York, **1998**.
- [14] D. Andrae, U. Haussermann, M. Dolg, H. Stoll, H. Preuss, *Theor. Chim. Acta* **1990**, 77, 123.
- [15] W. J. Hehre, R. Ditchfield, J. A. Pople, *J. Chem. Phys.* **1972**, 56, 2257.
- [16] P. C. Hariharan, J. A. Pople, *Chem. Phys. Lett.* **1972**, 16, 217.
- [17] a) C. Peng, P. Y. Ayala, H. B. Schlegel, M. J. Frisch, *J. Comput. Chem.* **1996**, 17, 49; b) H. B. Peng, C. Schlegel, *Isr. J. Chem.* **1994**, 34, 449.
- [18] a) V. Barone, M. Cossi, *J. Phys. Chem. A* **1998**, 102, 1995; b) M. Cossi, N. Rega, G. Scalmani, V. Barone, *J. Comput. Chem.* **2003**, 24, 669.
- [19] The CO stretching frequencies of their cationic carbonyl derivatives $[(C_6H_5)_2-2,6-(CH_2PCy_2)_2]Pd(CO)OTf$ ($\bar{\nu}_{CO}=2105\text{ cm}^{-1}$),^[20] $[(C_6H_5)_2-2,6-(OPiPr_2)_2]Pd(CO)]BF_4$ ($\bar{\nu}_{CO}=2141\text{ cm}^{-1}$), and $[(C_6H_5)[XP(piperidinyl)_2]_2Pd(CO)][BF_4]$ ($X=NH$, $\bar{\nu}_{CO}=2106\text{ cm}^{-1}$; $X=O$, $\bar{\nu}_{CO}=2133\text{ cm}^{-1}$) are indicative of the electron density at the metal centers.^[7]
- [20] Y. Jong Gook, S. Jung Min, L. Kap Duk, K. Sangha, P. Soonheum, *Bull. Korean Chem. Soc.* **1996**, 17, 311.
- [21] It turned out that this assumption was correct (e.g., see Figure 7).
- [22] J. Aydin, J. M. Larsson, N. Selander, K. J. Szabo, *Org. Lett.* **2009**, 11, 2852.
- [23] Chloride dissociation is relevant only in the first cycles, whereas bromide dissociation will be of importance at a later stage of catalysis (after complete chloride precipitation).
- [24] B. L. Shaw, S. D. Perera, *Chem. Commun.* **1998**, 1863.
- [25] For cationic reaction paths see below.
- [26] The phosphine-dissociation process of **4a** to form complexes of type **7a** is certainly accompanied by an energetic barrier ($TS_{4a/7a}$) due to subsequent rearrangements. However, since the energetic barrier is probably not very high, $TS_{4a/7a}$ was not calculated.
- [27] Moreover, the formation of **6a** is even more favored by initial dissociation of the chloride ligand from **1a** (to yield **2a**) and subsequent coordination of styrene (see below).
- [28] Ground-state energies of two exemplary isomeric structures of **8a** and **9a**, obtained from oxidative addition of either the vinyl C–H bond of styrene (to yield phenylethenyl hydride complex **8a**) or phenyl bromide (to give corresponding phenyl pincer complex **9a**) to **7a** were calculated (see Scheme 2 and Table 1). Product formation was strongly endothermic (the ground-state energies of **8a** and **9a** are 64.7 and 71.0 kcal mol⁻¹, respectively) and confirms that complexes of type **7** are not relevant for the catalytic cycle.
- [29] Since styrene adduct **6a** is present in the reaction mixture of Heck catalyses, its involvement in the catalytic mechanism seems plausible. In fact, complexes of type **6** were found to be the resting states of the catalytic cycle, providing facile access to cationic, T-shaped 14e⁻ complexes of type $[(2,6-C_6H_3(XPR_2)_2)Pd]^+$ (**2**), which are the key intermediates of the catalytic cycle (see below).
- [30] The energetic situation remains the same with phenyl iodide: optimized complex **2a** exhibits a ground-state, solvent-corrected energy which is 22.2 kcal mol⁻¹ higher than the ground-state energies of **1a** and phenyl iodide. The subsequent oxidative addition of phenyl iodide to **2a** to give cationic five-coordinate Pd^{IV} complex $[(2,6-C_6H_3[NHP(piperidinyl)_2]_2)Pd^+(C_6H_5)]^+$ with the phenyl ligand positioned *cis* to the aromatic unit of the pincer core is only slightly endothermic. $[(2,6-C_6H_3[NHP(piperidinyl)_2]_2)Pd^+(C_6H_5)]^+$ has a computed ground-state energy of 26.3 kcal mol⁻¹, which is 4.1 kcal mol⁻¹ higher than the sum of the ground-state energies of the reactants. The corresponding transition state is 16.3 kcal mol⁻¹ higher in energy than calculated for the isolated reactants and hence compares well with the results obtained for phenyl bromide.

Received: July 28, 2009

Revised: October 12, 2009

Published online: December 18, 2009